JOURNAL OF GUIDANCE, CONTROL, AND DYNAMICS
Vol. 28, No. 5, September–October 2005

Controller Design Using Standard Operator Model

Hiroshi Tokutake*
Osaka Prefecture University, Osaka 599-8531, Japan
and
Masayuki Sato†
Japan Aerospace Exploration Agency, Tokyo 181-0015, Japan

Manual tracking experiments were conducted to investigate aircraft operator responses. In these experiments, the operators attempted to track a random reference input. Afterward, the operators specified the workload required for the task. Using this information, operator models were identified and an operator control philosophy was derived. This philosophy was used to develop a controller design method with the standard operator model to reduce the workload. A standard operator model and controller were developed to allow the operator to control the plant easily. This design method was applied to a plant, and a reduction in workload was confirmed.

Nomenclature

e	=	tracking error
G_{re}	=	transfer function from reference input to tracking error
G_{ry}	=	transfer function from reference input to plant output
G_{uy}	=	transfer function from plant input to plant output (plant dynamics)
H_1, H_2	=	feedforward/feedback operator model
q	=	pitch rate
q_g	=	gust gradient component along the pitch axis
r	=	reference input
U_0	=	trimmed velocity
u	=	velocity change along the X axis
u_g	=	gust component along the X axis
u_K	=	controller output
u_P	=	plant input
u_1	=	output of feed-forward operator model
u_2	=	output of feedback operator model
y_H	=	input to feedback operator model from plant
y_K	=	input to controller from plant
$y[i]$	=	discretized operator output ($u_1 + u_2$)
w	=	velocity change along the Z axis
w_g	=	gust component along the Z axis
α	=	angle of attack
δ_{DLC}	=	direct lift control deflection angle
δ_{DLCc}	=	direct lift control deflection angle command
δ_e	=	elevator deflection angle
δ_{ec}	=	elevator deflection command
δ_t	=	power lever deflection
δ_{tc}	=	power lever deflection command
$\delta_1[i]$	=	discretized input to feed-forward operator model (r)
$\delta_2[i]$	=	discretized input to feedback operator model (y_H)
θ	=	pitch attitude

Introduction

PILOT-IN-THE-LOOP analysis is an effective tool for investigating aircraft operation. Reference 1 details the operation and an evaluation method for pilot rating. Pilot rating, which consists of operation workload (WL) and closed-loop performance, is determined from the operator's frequency response and a closed-loop system. A handling qualities metric is proposed in Ref. 2. This metric uses a structural model and agrees well with the experimental results. However, it is difficult to apply these handling qualities analyses to flight controller design. References 3–7 define a flight controller design using an eigenstructure assignment. Reference 8 incorporates CAP (control anticipation parameter)[9] and a systematic design method with modern control theory. These methods, though, are based on open-loop analysis and cannot be applied easily to advanced airplanes with complex dynamics.

This paper presents the results of manual control experiments with several dynamics. For each experiment, the operator workload was recorded and the operator's actions were modeled. Then a controller design method that guaranteed a low workload level was proposed and a manual control experiment was conducted to validate the proposed controller design.

Experiment

The manual control experiment involved having an operator track a target on a monitor, as shown in Fig. 1. The block diagram is shown in Fig. 2. The operator model contained two inputs and one output. The output on the monitor from the plant was disturbed in order to complete the two-block model fully. Sixteen controlled plants with a wide variety of pole and zero position characteristics were selected (Table 1). The marker position on the screen represented the plant output. The marker moved vertically in proportion to y'_P. The target moved vertically in proportion to r. The operator's goal was to try to maintain the target within the marker. The gear ratio was selected arbitrarily by the operator. The reference input r was white noise filtered with $\omega_{\mathrm{nr}}^2/(s^2 + 2\zeta_r\omega_{\mathrm{nr}}s + \omega_{\mathrm{nr}}^2)$, $\omega_{\mathrm{nr}} = 2$ rad/s, $\zeta_r = 0.8$, and disturbance d was white noise filtered with $\omega_{\mathrm{nd}}^2/(s^2 + 2\zeta_d\omega_{\mathrm{nd}}s + \omega_{\mathrm{nd}}^2)$, $\omega_{\mathrm{nd}} = 3$ rad/s, $\zeta_d = 0.25$, as shown in Fig. 3. In these experiments, the controlled dynamics was discretized at 50 Hz within the PC. The value 1 of the signals corresponds to 9.5 cm in the monitor.

Three operators were tested. Operator 1 was a 30-year-old male, operator 2 was a 20-year-old male, and operator 3 was a 23-year-old male. They were allowed to practice and select a suitable gear ratio. Then the experiment was carried out for 50 s and the workload, r, u_P, y_P, and y'_P were recorded. To estimate the workload precisely, benchmarks were established. The most difficult plant, D, was fixed as workload level 5, the easiest plant, F, was fixed as 1, and the middle plant, A, was fixed as 3. The operators determined their workloads by referencing these benchmark plants. The designated workloads for the plants, shown in Table 2, almost agreed.

Received 23 July 2004; revision received 28 September 2004; accepted for publication 16 October 2004.

*Research Associate, Department of Aerospace Engineering, Sakai. Member AIAA.

†Researcher, Advanced Control Research Group, Institute of Space Technology and Aeronautics, Mitaka.

Table 1 Controlled plant[a]

Plant	ω_n	ζ	p_1	p_2	z_1	z_2
A	1	0.1				
B	1	0.8				
C	1	1.5				
D	5	0.1				
E	5	0.8				
F	5	1.5				
G	10	0.1				
H	10	0.8				
I	10	1.5				
J	5	1.5	−5			
K	5	1.5	−10			
L	5	1.5	a_1	a_2		
M	5	1.5	b_1	b_2		
N	5	1.5	−5	−10		
O	5	1.5	b_1	b_2	a_1	a_2
P	5	1.5	b_1	b_2	−5	−10

[a] $a_1 = -5 + 5i$, $a_2 = -5 - 5i$, $b_1 = -10 + 10i$, $b_2 = -10 - 10i$, A∼I: $\omega_n^2/(s^2 + 2\zeta\omega_n s + \omega_n^2)$, J, K: $\omega_n^2/(s^2 + 2\zeta\omega_n s + \omega_n^2) \times -p_1/(s - p_1)$, L∼N: $\omega_n^2/(s^2 + 2\zeta\omega_n s + \omega_n^2) \times p_1 p_2/[(s - p_1)(s - p_2)]$, O, P: $\omega_n^2/(s^2 + 2\zeta\omega_n s + \omega_n^2) \times [(s - z_1)(s - z_2)]p_1 p_2/[(s - p_1)(s - p_2)]z_1 z_2$.

Table 2 Results (WL)

Plant	1	2	3	Plant	1	2	3
A	3	3	3	I	1	3	2
B	2	2	3	J	2	3	3
C	1	3	2	K	2	4	3
D	5	5	5	L	2	4	2
E	1	3	1	M	2	3	1
F	1	1	1	N	2	4	3
G	5	2	4	O	3	3	2
H	2	2	3	P	3	2	1

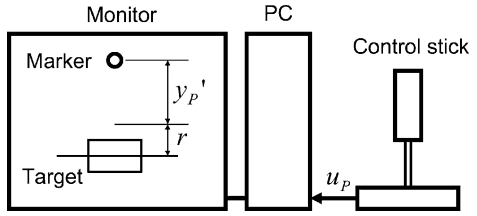

Fig. 1 Experimental apparatus.

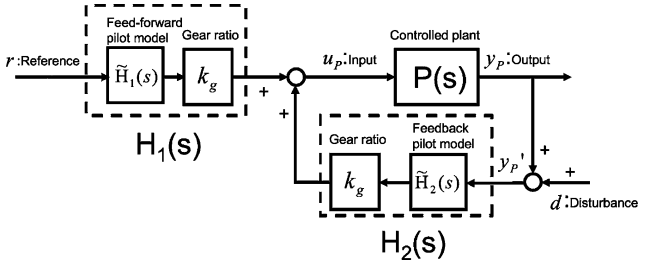

Fig. 2 Block diagram of tracking experiment.

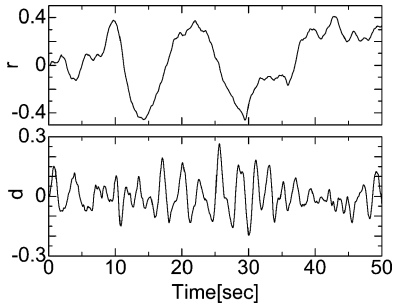

Fig. 3 Reference input and disturbance.

The following discrete model was proposed to identify the operator:

$$y[i+n] + a_{n-1}y[i+n-1] + \cdots + a_0 y[i] = b_m\delta_1[i+p] + \cdots + b_0\delta_1[i] + c_p\delta_2[i+m] + \cdots + c_0\delta_2[i] \quad (1)$$

Here, $y[i]$ is the output from the operator model and $\delta_1[i]$ and $\delta_2[i]$ are the inputs to the operator model. In general, the degree of model n is determined from the complexity and desired accuracy. In this research, a sufficiently high-order model was used to represent the operator dynamics precisely. By trial and error, $n = m = p = 5$ were selected. The least-squares method was used to identify the parameters in Eq. (1). This is a general tracking experiment. The operator model is based on an existing identification method and there have been several publications concerning operator models.[10–13]

Results

The frequency responses of operator models H_1 and H_2 for operator 1 performing plants A, D, F, and K, the open-loop transfer function G_{uy} from u_P to y_P, and the closed-loop transfer function G_{ry} from r to y_P are shown in Fig. 4. The operator's goal is to make $G_{ry} = 1$. The frequency response of G_{ry} coincides well with the wide bandwidth of G_{uy}, which agrees with the analysis of Ref. 1. At high frequencies, the gain and phase of G_{ry} decrease. This corresponds to an operator who does not track the reference input well. Next, the frequencies at which the operator reacts to the reference input were investigated using the closed-loop bandwidth. The tracking performance and closed-loop bandwidth, which was derived from the operator model, are shown in Table 3. The tracking performance is evaluated by using the following equation:

$$J = \sup_{0 \le \omega \le \omega_P} |G_{re}(j\omega)| \quad (2)$$

Here, G_{re} is a transfer function from r to $e = r - y_P$ and ω_P is the frequency with which the operator pays attention, which is set to 1.0 rad/s. If $r = \sin\omega_0 t$, where $\omega_0 < \omega_P$ is input as a reference, the output becomes $y_P = a_0 \sin(\omega_0 t + \phi_0)$, and $J < \epsilon$ guarantees $1 - \epsilon < a_0 < 1 + \epsilon$ and $-\cos^{-1}\sqrt{(1-\epsilon^2)} < \phi_0 < \cos^{-1}\sqrt{(1-\epsilon^2)}$. The proposed tracking performance index is a measure of gain and phase error between the reference input and the plant output. The bandwidth is defined as the frequencies where a gain of G_{ry} becomes smaller than −3 dB or the absolute value of the phase becomes larger than 30 deg. Table 3 indicates that the operator attempts to make the closed-loop bandwidth larger than 1 rad/s. This information justifies Eq. (2), which assumes that the operator senses the reference input at frequencies lower than 1 rad/s. Operators track the reference so that $J < 0.4$, regardless of the workload. Neal and Smith defined an operator model having a bandwidth of 3.5 rad/s (Ref. 1). Because

Table 3 Results (tracking performance and bandwidth)

	Tracking performance			Bandwidth rad/s		
Plant	1	2	3	1	2	3
A	0.40	0.39	0.39	0	1.1	0
B	0.65	0.66	0.86	0.8	0.9	0.6
C	0.74	0.79	0.83	0.6	0.7	0.6
D	0.47	0.5	0.79	1.3	0.8	0.4
E	0.40	0.43	0.59	1.3	1.1	0.7
F	0.43	0.45	0.57	1.2	1.1	0.8
G	0.51	0.39	0.7	1.0	1.4	0.5
H	0.33	0.25	0.5	1.7	2.1	1.0
I	0.17	0.27	0.38	2.7	1.7	1.4
J	0.36	0.34	0.71	1.5	1.3	0.6
K	0.18	0.43	0.72	2.0	1.1	0.6
L	0.32	0.45	0.55	1.6	1.1	0.9
M	0.46	0.37	0.61	1.1	1.2	0.8
N	0.37	0.47	0.65	1.3	1.0	0.7
O	0.32	0.21	0.48	1.6	1.6	1.0
P	0.32	0.27	0.42	1.7	1.7	1.2

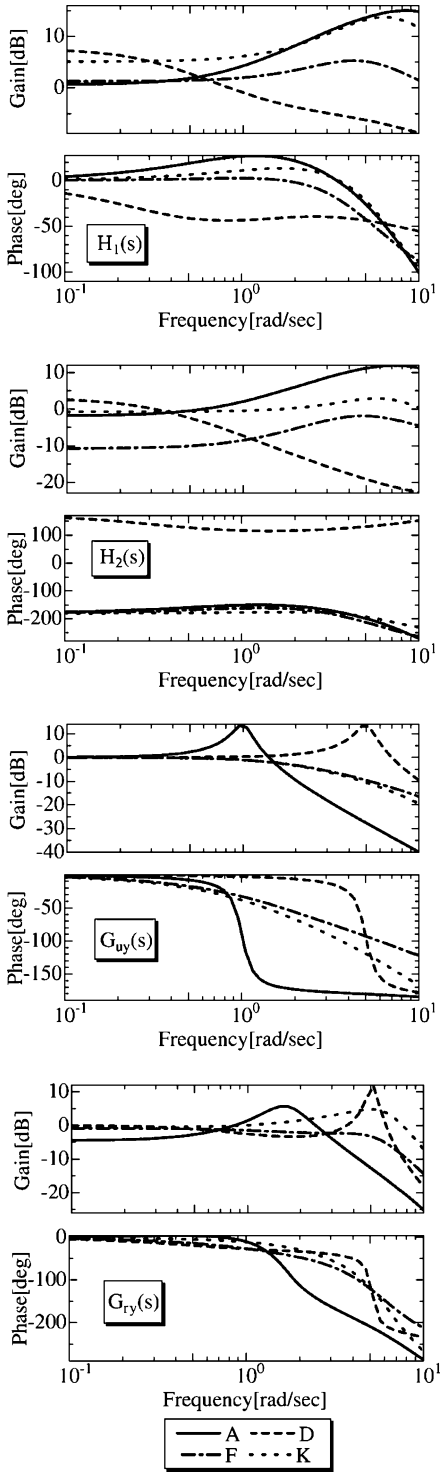

Fig. 4 Frequency responses.

this research defined bandwidth using smaller phase, the results do not conflict with Neal and Smith's result.

Reference 1 shows the relationship between pilot rating and a one-block operator model. The pilot rating contains closed-loop performance and workload information, and so this operator model contains some workload information. In this research, however, a two-block operator model is used to model operator dynamics precisely. The controller design method, presented in the next section, was developed to guarantee a low workload.

Controller Design Guaranteeing Workload

The following operation philosophy was derived from the operation experiment results. The operator is modeled as the solutions to the following optimization problem:

$$\begin{aligned} &\underset{H_1,H_2}{\text{minimize}} \quad \text{WL} \quad \text{s.t. } J < \epsilon_{\text{tol}} \\ &\epsilon_{\text{tol}} = 0.4 \end{aligned} \tag{3}$$

The analysis of experimental results shows that a well-motivated operator can attain a certain tracking performance. Equation (3) is a formulation of this conclusion. However, the operator model that attains this certain tracking performance cannot be uniquely determined. Therefore, it is assumed that the operator will choose the smallest workload model in the solution set that attains the given performance. It is also assumed that the operator is well trained.

The estimation of operation workload is not the focus of this research. Instead, the controller design method that guarantees a certain workload level is shown via that standard operator model. Let the feedforward/feedback operator models be arbitrarily designated as H_{1s} and H_{2s}. These are referred to as the standard operator model. It is assumed that the operator model determines the workload level. Let the workload level of given standard operator model be α, the controlled plant be P, and the well-motivated and trained operator models be H_1 and H_2. The theorem is derived in the next section.

Theorem 1: If

$$\sup_{0 \le \omega \le \omega_P} \left| \frac{1 - P(H_{1s} + H_{2s})}{1 - PH_{2s}} \right| < \epsilon_{\text{tol}} \tag{4}$$

is satisfied, the workload level of H_1 and H_2 is smaller than α.

Proof: It is clear from $G_{re} = (1 - P(H_1 + H_2))/(1 - PH_2)$ and Eq. (3). □

When the controlled plant is designed to satisfy Eq. (4) for the standard operator model, good tracking performance can be guaranteed with a smaller workload level than specified.

The desired plant dynamics can be obtained with an appropriate controller. The controller design method that satisfies Eq. (4) is shown in a closed-loop system in Fig. 5. In this figure, y_H is the plant output that the operator senses and y_K is the plant output that is input into the controller. The state-space representations of controlled plant P, the standard operator model H_{1s} and H_{2s}, and the weighting function W, which restricts bandwidth, are given as follows.

Controlled plant P:

$$\dot{x}_P = A_P x_P + B_P u_P, \qquad y_H = C_P x_P, \qquad y_K = C_{PK} x_P$$

Standard operator model H_{1s}:

$$\dot{x}_{H1} = A_{H1} x_{H1} + B_{H1} r, \qquad u_1 = C_{H1} x_{H1} + D_{H1} r$$

Standard operator model H_{2s}:

$$\dot{x}_{H2} = A_{H2} x_{H2} + B_{H2} y_H, \qquad u_2 = C_{H2} x_{H2} + D_{H2} y_H$$

Weighting function W:

$$\dot{x}_W = A_W x_W + B_W e, \qquad z = C_W x_W + D_W e$$

The generalized plant is defined as follows.
Generalized plant:

$$\dot{x} = Ax + B_1 r + B_2 u_K, \qquad z = C_1 x + D_{11} r + D_{12} u_K$$

$$y_K = C_2 x + D_{21} r + D_{22} u_K$$

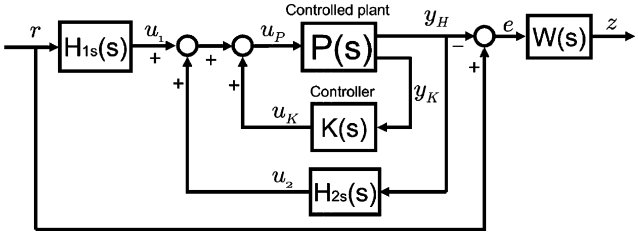

Fig. 5 Closed-loop system.

Here,

$$x = \begin{bmatrix} x_P^T & x_{H1}^T & x_{H2}^T & x_W^T \end{bmatrix}^T$$

$$A = \begin{bmatrix} A_P + B_P D_{H2} C_P & B_P C_{H1} & B_P C_{H2} & 0 \\ 0 & A_{H1} & 0 & 0 \\ B_{H2} C_P & 0 & A_{H2} & 0 \\ -B_W C_P & 0 & 0 & A_W \end{bmatrix}$$

$$B_1 = \begin{bmatrix} B_P D_{H1} \\ B_{H1} \\ 0 \\ B_W \end{bmatrix}, \qquad B_2 = \begin{bmatrix} B_P \\ 0 \\ 0 \\ 0 \end{bmatrix}$$

$$C_1 = [-D_W C_P \quad 0 \quad 0 \quad C_W]$$

$$C_2 = [C_{PK} \quad 0 \quad 0 \quad 0]$$

$$D_{11} = D_W, \qquad D_{12} = 0, \qquad D_{21} = 0, \qquad D_{22} = 0$$

Let the transfer function from r to z be G_{rz}. The weighting function is selected so that $W \simeq 1$ for a frequency of $\omega < \omega_P$ and $|W| \ll 1$ for a frequency of $\omega \geq \omega_P$. The controller design requirement that satisfies Eq. (4) is as follows:

1) Find the controller $u_K = K(s) y_K$ s.t. $\|G_{rz}\|_\infty < \epsilon_{\text{tol}}$.

The controller design that ensures a low workload level results in H_∞ suboptimal problems. The problem's numerous design methods are shown and the full-order controller can be obtained easily.

Design Example

Application to Manual Control Experiment

The design example detailed in this section exhibits the workload level improvements. This example uses plant D, which resulted in the worst workload level in the manual control experiment for the standard operator model, and operator 1, the best workload level of which was plant F. The operator model was defined as a second-order model [$n = m = p = 2$ in Eq. (1)] to decrease the degree of the controller. The weighting function is $W(s) = 1/(s+1)$ and $C_{PK} = I$. Thus, the controller that minimizes $\|G_{rz}\|_\infty$ can be obtained using the method described in Ref. 14. The controller obtained in this example is

$$K(s) = C_K (sI - A_K)^{-1} B_K + D_K$$

$$A_K = \begin{bmatrix} 2.44 & -11.39 & -1.47 & 3.59 & 2.56 & 36.36 & -8.07 \\ 3.68 & -58.6 & -14.32 & -4.08 & -0.85 & -12.25 & 4.92 \\ 1.16 & -15.76 & -3.51 & 5.61 & 0.78 & 5.01 & -1.1 \\ -5.94 & 64.51 & 7.05 & -86.45 & -9.03 & -67.08 & 24.52 \\ -1.45 & -27.65 & -5.12 & -11.12 & 13.96 & 86.55 & 13.46 \\ 10.61 & 12.66 & 0.34 & -27.67 & -16.86 & -23.5 & -26.96 \\ 30.03 & -36.25 & -7.4 & -1.25 & -26.76 & 32.47 & -80.8 \end{bmatrix}$$

$$B_K = \begin{bmatrix} -35.4 & 48.5 \\ 109.41 & -2.36 \\ 20.8 & 7.96 \\ -45.55 & -9.03 \\ -77.6 & 136.71 \\ -25.77 & 17.77 \\ -45.18 & 99.86 \end{bmatrix}$$

$$C_K = [-4.01 \quad 0.53 \quad 0.14 \quad 0.35 \quad 6.36 \quad 1.47 \quad 2.62]$$

$$D_K = [0 \quad 0]$$

This controller attained $\|G_{rz}\|_\infty = 0.29$ while satisfying design requirement 1. The manual control experiment for plant D was then carried out using the new controller. Operator 1 labeled the workload level as level 1. The frequency responses of the operator model, the operated plant, and the closed-loop system for plant D with the controller and plants D and F without the controller are shown in Fig. 6. As is evident in the figure, the operator model and the closed-loop system for D with the new controller are similar to those for plant F without the controller. This indicates that the operator controls plant D with the controller in the same way as plant F. In addition, the peak of the closed-loop gain also decreased when the new controller is employed.

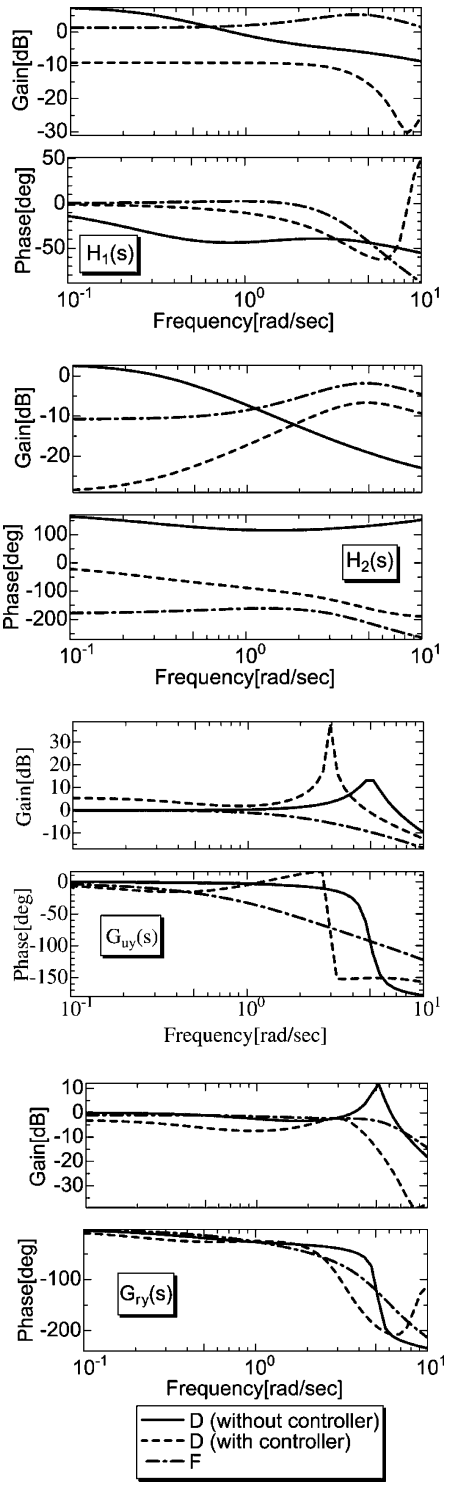

Fig. 6 Results (frequency responses).

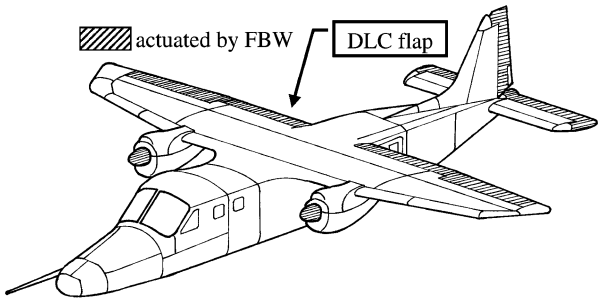

Fig. 7 MuPAL-α.

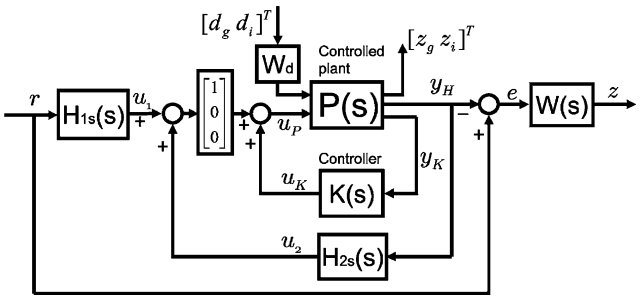

Fig. 8 Pilot-airplane.

Application to Airplane

The proposed method was then applied to flight controller design. The airplane used for this experiment is the Multi-Purpose Aviation Laboratory (MuPAL-α) flying at an elevation of 5000 ft with $U_0 = 66.5$ m/s (Fig. 7). MuPAL-α has three control inputs for longitudinal dynamics: elevator angle δ_e, direct lift control (DLC) angle δ_{DLC}, and power lever deflection δ_t.

The following requirements must be satisfied: 1) good handling qualities, 2) decreased pitch rate response to gust disturbance, and 3) robust stability to multiplicative input uncertainty.

The first requirement was satisfied by the proposed method and the remaining requirements were satisfied by the H_∞ controller. The closed-loop schematic is shown in Fig. 8. In this design, d_g is the gust input, d_i is the output from the uncertainty, z_g is the pitch rate, and z_i is the input to the uncertainty. First, the pitch command flight control is considered. Let the reference input r be the pitch angle θ, the output to controller y_K be θ, and the input to the feedback pilot model be θ.

The resulting controlled plant and weighting function are as follows:

$$\dot{x}_L = A_L x_L + B_{dg} d_g + B_{di} d_i + B_L u_L, \qquad y_H = \theta, \qquad y_K = \theta$$

$$A_L = \begin{bmatrix} -0.0162 & 0.172 & -6.09 & -9.76 & 0.466 \\ -0.183 & -1.09 & 64.5 & -0.915 & -4.94 \\ 0.00799 & -0.0692 & -1.90 & 0.00667 & -4.25 \\ 0 & 0 & 1 & 0 & 0 \\ 0 & 0 & 0 & 0 & -9.79 \end{bmatrix}$$

$$B_L = \begin{bmatrix} 0 & 0.336 & 0.0193 \\ 0 & -6.10 & -0.00427 \\ 0 & 0.760 & 0.000488 \\ 0 & 0 & 0 \\ 6.86 & 0 & 0 \end{bmatrix}$$

$$B_{Ldg} = \begin{bmatrix} -0.0162 & 0.172 & 0.0781 \\ -0.183 & -1.09 & -0.828 \\ 0.00799 & -0.0692 & -0.943 \\ 0 & 0 & 0 \\ 0 & 0 & 0 \end{bmatrix}$$

$$B_{di} = B_L \tag{5}$$

$$W(s) = \frac{1}{s+1} \tag{6}$$

$$W_d(s) = I \tag{7}$$

$$x_L = [u \quad w \quad q \quad \theta \quad \delta_e]^T, \qquad d_g = [u_g \quad w_g \quad q_g]^T$$

$$u_L = [\delta_{ec} \quad \delta_{\mathrm{DLCc}} \quad \delta_{tc}]^T$$

The elevator dynamics are modeled as a first-order lag system. The H_∞ controller that minimizes the H_∞ norm of the transfer function from $\hat{d}$ to $\hat{z}$ is obtained. Here, $\hat{d} = [r \ \ d_g \ \ d_i]^T$, $\hat{z} = [z \ \ z_g \ \ z_i]^T$.

The following standard pilot is selected:

$$H_{1s} = \frac{K_{H1}}{T_{H1}s + 1}, \qquad H_{2s} = -H_{1s}, \qquad K_{H1} = -3, \qquad T_{H1} = 1$$

This model is selected using the result of tracking experiments. In the case of actual flight controller design, it must be selected carefully, taking account of task, reference input, and other requirements.

The controller is

$$\dot{x}_K = A_K x_K + B_K y_K, \qquad u_K = C_K x_K + D_K y_K$$

$$A_K = \begin{bmatrix} -1.02 & -1.97 & -1.10 & -3.82 & 0.0293 & 1.72 & -1.17 & -1.35 \\ -0.0295 & 3.81 & 4.45 & 19.3 & -0.114 & 4.06 & -9.35 & -3.97 \\ 0.135 & 0.659 & -1.18 & -2.69 & 0.0001 & -5.08 & 6.82 & 4.53 \\ 0.627 & 0.694 & 0.354 & -5.04 & -0.0349 & -12.5 & 16.6 & 10.5 \\ 0.0172 & 0.0073 & 0.0489 & 0.120 & -0.0303 & -0.185 & 0.454 & 0.0865 \\ 0.662 & 17.8 & 9.47 & 28.9 & -0.327 & -26.0 & 23.4 & 14.9 \\ 3.12 & -73.8 & -24.9 & -94.3 & 0.351 & 43.5 & -24.8 & -14.6 \\ -1.65 & 22.9 & 5.71 & 26.8 & -0.0700 & -3.51 & -6.38 & -32.6 \end{bmatrix}, \qquad B_K = \begin{bmatrix} 7.14 \\ -30.6 \\ -0.542 \\ -7.67 \\ -3.76 \\ -92.1 \\ 256 \\ -68.81 \end{bmatrix}$$

$$C_K = \begin{bmatrix} 0.156 & -0.664 & -0.0358 & -0.326 & -0.0207 & -3.31 & 4.51 & 4.66 \\ -0.0647 & 0.213 & -0.0157 & 0.0308 & 0.0100 & 1.13 & -1.41 & -1.02 \\ -0.00 & 0.0001 & 0.00 & 0.00 & -0.0001 & 0.0007 & -0.0009 & -0.0004 \end{bmatrix}, \qquad D_K = \begin{bmatrix} 0 \\ 0 \\ 0 \end{bmatrix}$$

The obtained controller attains $\|T_{rz}\|_\infty = 0.6086$, $\|T_{dzg}\|_\infty = 0.1841$, and $\|T_{dzi}\|_\infty = 1.4770$. Here, T_{rz}, T_{dzg}, and T_{dzi} are the transfer functions from r to z, from d_g to z_g, and from d_i to z_i, respectively. $\|T_{rz}\|_\infty = 1.2695$, and $\|T_{dzg}\|_\infty = 1.4770$ are satisfied

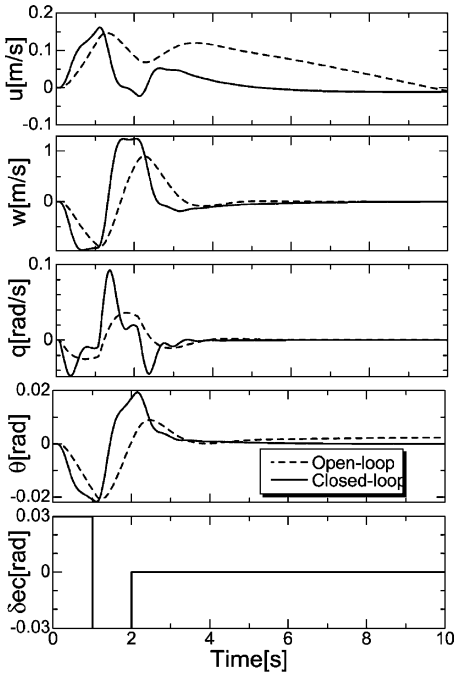

Fig. 9 Doublet responses.

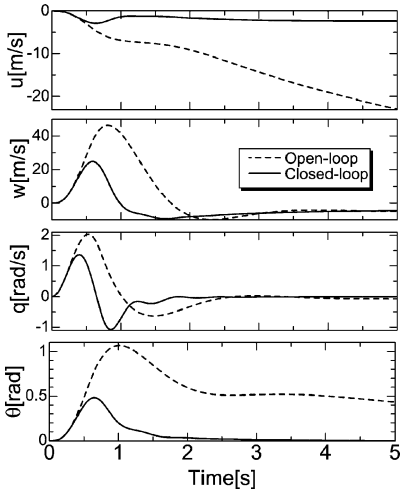

Fig. 10 Gust responses.

for the open-loop system. Therefore, the handling qualities of the controller improve and the response to gusts decreases.

Next, the time responses are investigated. Figure 9 shows the responses to a doublet elevator command input. The controller was designed so that pilot can track the pitch command without difficulty. These responses verify the validity of the design. Figure 10 shows the gust responses. The following gust parameters were used in this example:

$$[t < \pi/\omega_{\text{nscl}}], \qquad u_g = 0, \qquad w_g = (V_m/2)\{1 - \cos(\omega_{\text{nscl}} t)\}$$

$$q_g = -(V_m \omega_{\text{nscl}}/2)\sin(\omega_{\text{nscl}} t), \qquad [t \geq \pi/\omega_{\text{nscl}}]$$

$$u_g = 0 \; w_g = V_m, \qquad q_g = 0$$

Here, ω_{nscl} is the closed-loop natural frequency, $d_g = [u_g \;\; w_g \;\; q_g]^T$, and $V_m = 4.3$ m/s is the true air speed.

Because the frequency of gusts is equal to the short-period mode frequency of the closed-loop system, the response becomes large. However, the closed-loop system responses are smaller than those for the open-loop system.

Conclusion

Manual tracking experiments were performed to define two-block operator models. The two-block model anticipates an operator's actions using feedback and feedforward processes. The purpose of the controller was to achieve a low operator workload while attaining high tracking performance. The obtained controller successfully attained high closed-loop performance at an appropriate workload level. Tracking experiments were then conducted with a controller designed by the proposed method, and the results verified an overall reduction in workload level. Next, the proposed method was applied to a flight controller. The controller was successfully designed to minimize the workload level of the pitch tracking operation while reducing the gust response and stabilizing the aircraft relative to plant uncertainty.

References

[1]Neal, T., and Smith, R., "An In-Flight Investigation to Develop Control System Design Criteria for Fighter Airplanes," AFFDL-TR-70-74, 1 and 2, Wright–Patterson AFB, OH, 1970.

[2]Hess, R. A., "Methodology for the Analytical Assessment of Aircraft Handling Qualities," *Control and Dynamic Systems*, Vol. 33, April 1990, pp. 129–149.

[3]Andry, A. N., Jr., Shapiro, E. Y., and Chung, J. C., "Eigenstructure Assignment for Lin-ear Systems," *IEEE Transactions on Aerospace and Electronic Systems*, Vol. AES-19, No. 5, 1983, pp. 711–729.

[4]Sobel, K. M., Shapiro, E. Y., and Andry, A. N., Jr., "Eigenstructure Assignment," *International Journal of Control*, Vol. 59, No. 1, 1994, pp. 13–37.

[5]Yu, W., and Sobel, K. M., "Robust Eigenstructure Assignment with Structured State Space Uncertainty," *Journal of Guidance, Control, and Dynamics*, Vol. 14, No. 3, 1991, pp. 621–628.

[6]Satoh, A., and Sugimoto, K., "Partial Eigenstructure Assignment Approach for Robust Flight Control," *Journal of Guidance, Control, and Dynamics*, Vol. 27, No. 1, 2004, pp. 145–150.

[7]Tokutake, H., "Robust Flight Control Design with Eigenstructure Assignment," *Preprints of 15th IFAC Symposium on Automatic Control in Aerospace*, International Federation of Automatic Control, Laxenburg, Austria, 2001, pp. 191–196.

[8]Tokutake, H., Sato, M., and Satoh, A., "Robust Flight Controller Design That Takes into Account Handling Quality," *Journal of Guidance, Control, and Dynamics*, Vol. 28, No. 1, 2005, pp. 71–77.

[9]Chalk, C. R., "Simulator Investigation of the Effect of L_α and True Speed on Longitudinal Handling Qualities," *Journal of Aircraft*, Vol. 1, No. 6, 1964, pp. 335–344.

[10]McRuer, D. T., and Krendel, E. S., "Dynamic Response of Human Operators," Wright–Patterson AFB, OH, WADC-TR-56-524, Oct. 1957.

[11]McRuer, D. T., and Krendel, E. S., "Mathmatical Models of Human Pilot Behavior," AGARD AG-188, Jan. 1974.

[12]McRuer, D., "Human Dynamics in Man–Machine Systems," *Automatica*, Vol. 16, 1980, pp. 237–253.

[13]Hess, R. A., "Feedback Control Models—Manual Control and Tracking," *Handbook of Human Factors and Ergonomics*, edited by G. Salvendy, Wiley, New York, 1997, pp. 1279–1294.

[14]Gahinet, P., and Apkarian, P., "A Linear Matrix Inequality Approach to H_∞ Control," *International Journal of Robust and Nonlinear Control*, Vol. 4, 1994, pp. 421–448.